Chalmers Publication Library

Copyright Notice

©2010 IEEE. Personal use of this material is permitted. However, permission to reprint/republish this material for advertising or promotional purposes or for creating new collective works for resale or redistribution to servers or lists, or to reuse any copyrighted component of this work in other works must be obtained from the IEEE.

This document was downloaded from Chalmers Publication Library (http://publications.lib.chalmers.se/), where it is available in accordance with the IEEE PSPB Operations Manual, amended 19 Nov. 2010, Sec. 8.1.9 (http://www.ieee.org/documents/opsmanual.pdf)

(Article begins on next page)

NLOS Identification and Mitigation for Localization Based on UWB Experimental Data

Stefano Maranò, *Student Member, IEEE*, Wesley M. Gifford, *Student Member, IEEE*, Henk Wymeersch, *Member, IEEE*, Moe Z. Win, *Fellow, IEEE*

***Abstract*—Sensor networks can benefit greatly from location-awareness, since it allows information gathered by the sensors to be tied to their physical locations. Ultra-wide bandwidth (UWB) transmission is a promising technology for location-aware sensor networks, due to its power efficiency, fine delay resolution, and robust operation in harsh environments. However, the presence of walls and other obstacles present a significant challenge in terms of localization, as they can result in positively biased distance estimates. We have performed an extensive indoor measurement campaign with FCC-compliant UWB radios to quantify the effect of non-line-of-sight (NLOS) propagation. From these channel pulse responses, we extract features that are representative of the propagation conditions. We then develop classification and regression algorithms based on machine learning techniques, which are capable of: (i) assessing whether a signal was transmitted in LOS or NLOS conditions; and (ii) reducing ranging error caused by NLOS conditions. We evaluate the resulting performance through Monte Carlo simulations and compare with existing techniques. In contrast to common probabilistic approaches that require statistical models of the features, the proposed optimization-based approach is more robust against modelling errors.**

***Index Terms*—Localization, UWB, NLOS Identification, NLOS Mitigation, Support Vector Machine.**

I. Introduction

LOCATION-awareness is fast becoming a fundamental aspect of wireless sensor networks and will enable a myriad of applications, in both the commercial and the military sectors [1], [2]. Ultra-wide bandwidth (UWB) transmission provides robust signaling, as well as through-wall propagation and high-resolution ranging capabilities [3]–[12]. Therefore, UWB represents a promising technology for localization applications in harsh environments and accuracy-critical applications [13]–[20]. In practical scenarios, however, a number of challenges remain before UWB localization and communication can be deployed. These include signal acquisition [21], [22], multi-user interference [23], [24], multipath effects [25]–[28], and non-line-of-sight (NLOS) propagation. The latter issue is especially critical [15]–[17], [20] for high-resolution localization systems, since NLOS propagation introduces positive biases in distance estimation algorithms, thus seriously affecting the localization performance. Typical harsh environments such as enclosed areas, urban canyons, or under tree canopies inherently have a high occurrence of NLOS situations. It is therefore critical to understand the impact of NLOS conditions on localization systems and to develop techniques that mitigate their effects.

There are several ways to deal with ranging bias in NLOS conditions, which we classify as *identification* and *mitigation*. NLOS identification attempts to distinguish between LOS and NLOS conditions, and is commonly based on range estimates [29]–[31] or on the channel pulse response (CPR) [32], [33]. Recent, detailed overviews of NLOS identification techniques can be found in [30], [34]. NLOS mitigation goes beyond identification and attempts to counter the positive bias introduced in the NLOS signals. Several techniques [35]–[39] rely on a number of redundant range estimates, both LOS and NLOS, in order to reduce the impact of NLOS range estimates on the estimated agent position. In [40]–[42] the geometry of the environment is explicitly taken into account to cope with NLOS situations. Other approaches, such as [43], attempt to detect the earliest path in the CPR in order to better estimate the TOA in NLOS conditions. Therefore, when the direct path is detectable, the ranging error is reduced [34]. Comprehensive overviews of NLOS mitigation techniques can be found in [34], [44].

The main drawbacks of existing NLOS identification and mitigation techniques are: (i) loss of information due to the direct use of ranges instead of the CPRs; (ii) latency incurred during the collection of range estimates to establish a history; and (iii) difficulty in determining the joint probability distributions of the features required by many statistical approaches.

In this paper, we consider an optimization-based approach. In particular, we propose the use of *non-parametric machine learning techniques* to perform NLOS identification and NLOS mitigation. Hence, they do not require a statistical characterization of LOS and NLOS channels and can perform identification and mitigation under a common framework. The main contributions of this paper are as follows:

- characterization of differences in the CPRs under LOS and NLOS conditions based on an extensive indoor measurement campaign with FCC-compliant UWB radios;
- identification of novel features extracted from the CPR that capture the salient properties in LOS and NLOS

Manuscript received May 15, 2009; revised February 15, 2010. This research was supported, in part, by the National Science Foundation under Grants ECCS-0636519 and ECCS-0901034, the Office of Naval Research Presidential Early Career Award for Scientists and Engineers (PECASE) N00014-09-1-0435, the Defense University Research Instrumentation Program under Grant N00014-08-1-0826, and the MIT Institute for Soldier Nanotechnologies.

Stefano Maranò was with Laboratory for Information and Decision Systems (LIDS), Massachusetts Institute of Technology (MIT), and is now with the Swiss Seismological Service, ETH Zürich, Zürich, Switzerland (e-mail: stefano.marano@sed.ethz.ch). Henk Wymeersch was with LIDS, MIT, and is now with Chalmers University of Technology, Göteborg, Sweden (e-mail: henkw@chalmers.se). Wesley M. Gifford and Moe Z. Win are with LIDS, MIT, Cambridge, MA 02139 USA (e-mail: wgifford@mit.edu, moewin@mit.edu).

conditions;
- demonstration that a support vector machine (SVM) classifier can be used to distinguish between LOS and NLOS conditions, without the need for statistical modeling of the features under either condition; and
- development of SVM regressor-based techniques to mitigate the ranging bias in NLOS situations, again without the need for statistical modeling of the features under either condition.

The remainder of the paper is organized as follows. In Section II, we introduce the system model, problem statement, and describe the effect of NLOS conditions on ranging. In Section III, we describe the equipment and methodologies of the LOS/NLOS measurement campaign and its contribution to this work. The proposed techniques for identification and mitigation are described in Section IV, while different strategies for incorporating the proposed techniques within any localization system are discussed in Section V. Numerical performance results are provided in Section VI, and we draw our conclusions in Section VII.

II. Problem Statement and System Model

In this section, we describe the ranging and localization algorithm, and demonstrate the need for NLOS identification and mitigation.

A. Single-node Localization

A network consists of two types of nodes: *anchors* are nodes with known positions, while *agents* are nodes with unknown positions. For notational convenience, we consider the point of view of a single agent, with unknown position $\mathbf{p}$, surrounded by N_b anchors, with positions, $\mathbf{p}_i$, $i = 1, \ldots, N_\mathrm{b}$. The distance between the agent and anchor i is $d_i = \|\mathbf{p} - \mathbf{p}_i\|$.

The agent estimates the distance between itself and the anchors, using a ranging protocol. We denote the estimated distance between the agent and anchor i by $\hat{d}_i$, the ranging error by $\varepsilon_i = \hat{d}_i - d_i$, the estimate of the ranging error by $\hat{\varepsilon}_i$, the channel condition between the agent and anchor i by $\lambda_i \in \{\mathrm{LOS}, \mathrm{NLOS}\}$, and the estimate of the channel condition by $\hat{\lambda}_i$. The mitigated distance estimate of d_i is $\hat{d}_i^\mathrm{m} = \hat{d}_i - \hat{\varepsilon}_i$. The residual ranging error after mitigation is defined as $\varepsilon_i^\mathrm{m} = \hat{d}_i^\mathrm{m} - d_i$.

Given a set of at least three distance estimates, the agent will then determine its position. While there are numerous positioning algorithms, we focus on the least squares (LS) criterion, due to its simplicity and because it makes no assumptions regarding ranging errors. The agent can infer its position by minimizing the LS cost function

$$\hat{\mathbf{p}} = \arg\min_{\mathbf{p}} \sum_{(\mathbf{p}_i, \hat{d}_i) \in \mathcal{S}} \left(\hat{d}_i - \|\mathbf{p} - \mathbf{p}_i\| \right)^2 . \qquad (1)$$

Note that we have introduced the concept of the set of *useful neighbors* $\mathcal{S}$, consisting of couples $\left(\mathbf{p}_i, \hat{d}_i\right)$. The optimization problem (1) can be solved numerically using steepest descent.

B. Sources of Error

The localization algorithm will lead to erroneous results when the ranging errors are large. In practice the estimated distances are not equal to the true distances, because of a number of effects including thermal noise, multipath propagation, interference, and ranging algorithm inaccuracies. Additionally, the direct path between requester and responder may be obstructed, leading to NLOS propagation. In NLOS conditions, the direct path is either attenuated due to through-material propagation, or completely blocked. In the former case, the distance estimates will be positively biased due to the reduced propagation speed (i.e., less than the expected speed of light, c). In the latter case the distance estimate is also positively biased, as it corresponds to a reflected path. These bias effects can be accounted for in either the ranging or localization phase.

In the remainder of this paper, we focus on techniques that *identify* and *mitigate* the effects of NLOS signals during the ranging phase. In NLOS identification, the terms in (1) corresponding to NLOS distance estimates are omitted. In NLOS mitigation, the distance estimates corresponding to NLOS signals are corrected for improved accuracy. The localization algorithm can then adopt different strategies, depending on the quality and the quantity of available range estimates.

III. Experimental Activities

This section describes the UWB LOS/NLOS measurement campaign performed at the Massachusetts Institute of Technology by the Wireless Communication and Network Sciences Laboratory during Fall 2007.

A. Overview

The aim of this experimental effort is to build a large database containing a variety of propagation conditions in the indoor office environment. The measurements were made using two FCC-compliant UWB radios. These radios represent off-the-shelf transceivers and therefore an appropriate benchmark for developing techniques using currently available technology. The primary focus is to characterize the effects of obstructions. Thus, measurement positions (see Fig. 1) were chosen such that half of the collected waveforms were captured in NLOS conditions. The distance between transmitter and receiver varies widely, from roughly 0.6 m up to 18 m, to capture a variety of operating conditions.

Several offices, hallways, one laboratory, and a large lobby constitute the physical setting of this campaign. The scope of the campaign matches the so called *indoor office* environment [12]. While the campaign was conducted in one particular environment, because of the large number of measurements and the variety of propagation scenarios encountered, we expect that our results are applicable in other indoor office environments. The physical arrangement of the campaign is depicted in Fig. 1.

In each measurement location, the received waveform and the associated range estimate, as well as the actual distance are recorded. The waveforms are then post-processed in order to reduce dependencies on the specific algorithm and hardware,

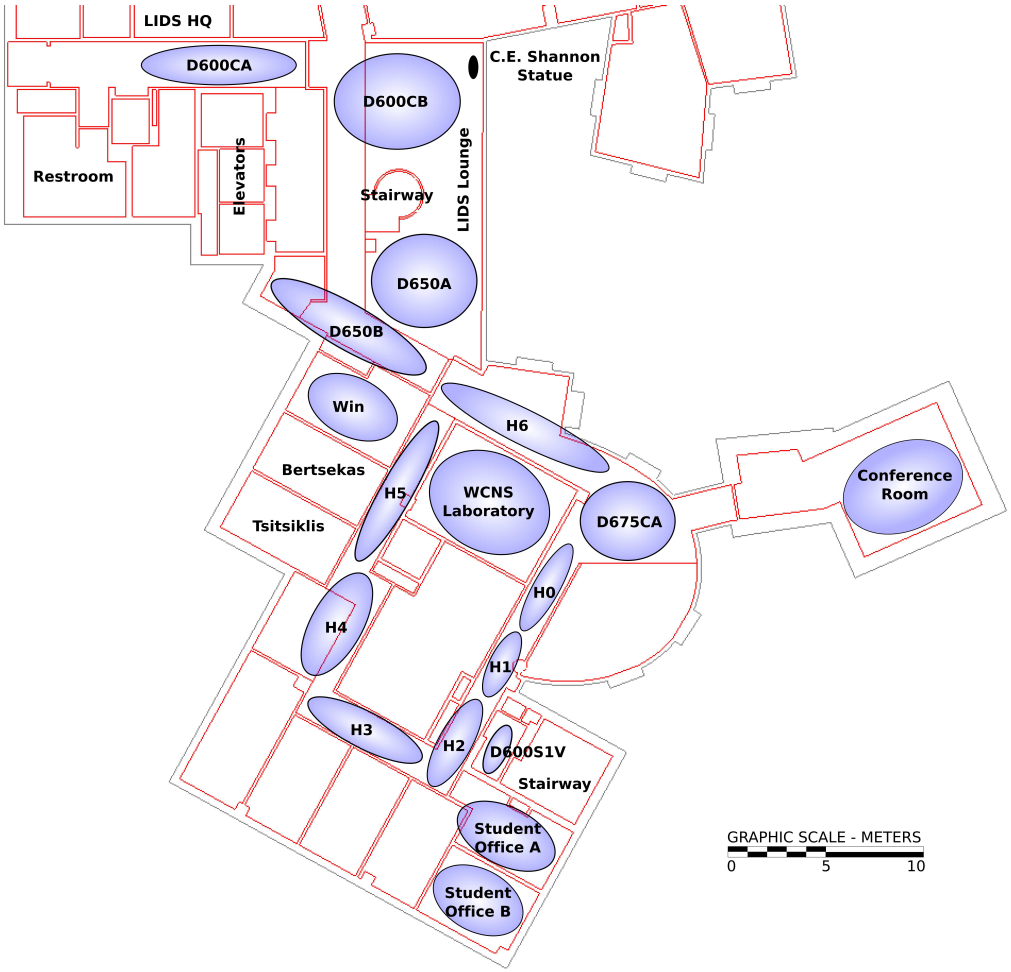

Fig. 1. Measurements were taken in clusters over several different rooms and hallways to capture different propagation conditions.

e.g., on the leading edge detection (LED) algorithm embedded in the radios.

B. Experimental Apparatus

The commercially-available radios used during the data collection process are capable of performing communications and ranging using UWB signals. The radio complies with the emission limit set forth by the FCC [45]. Specifically, the 10 dB bandwidth spans from 3.1 GHz to 6.3 GHz. The radio is equipped with a bottom fed planar elliptical antenna. This type of dipole antenna is reported to be well matched and radiation efficient. Most importantly, it is omni-directional and thus suited for ad-hoc networks with arbitrary azimuthal orientation [46]. Each radio is mounted on the top of a plastic cart at a height of 90 cm above the ground. The radios perform a round-trip time-of-arrival (RTOA) ranging protocol[1] and are capable of capturing waveforms while performing the ranging procedure. Each waveform $r(t)$ captured at the receiving radio is sampled at 41.3 ps over an observation window of 190 ns.

[1]RTOA allows ranging between two radios *without* a common time reference; and thus alleviates the need for network synchronization.

Fig. 2. The measurement setup for collecting waveforms between D675CA and H6 around the corner of the WCNS Laboratory.

C. Measurement Arrangement

Measurements were taken at more than one hundred points in the considered area. A map, depicting the topological organization of the clusters within the building, is shown in Fig. 1, and a typical measurement scenario is shown in Fig. 2. Points are placed randomly, but are restricted to areas

which are accessible by the carts. The measurement points are grouped into non-overlapping clusters, i.e., each point only belongs to a single cluster. Typically, a cluster corresponds to a room or a region of a hallway. Within each cluster, measurements between every possible pair of points were captured. When two clusters were within transmission range, every inter-cluster measurement was collected as well. Overall, more than one thousand unique point-to-point measurements were performed. For each pair of points, several received waveforms and distance estimates are recorded, along with the actual distance. During each measurement the radios remain stationary and care is taken to limit movement of other objects in the nearby surroundings.

D. Database

Using the measurements collected during the measurement phase, a database was created and used to develop and evaluate the proposed identification and mitigation techniques. It includes 1024 measurements consisting of 512 waveforms captured in the LOS condition and 512 waveforms captured in the NLOS condition. The term LOS is used to denote the existence of a *visual* path between transmitter and receiver, i.e., a measurement is labeled as LOS when the straight line between the transmitting and receiving antenna is unobstructed. The ranging estimate was obtained by an RTOA algorithm embedded on the radio. The actual position of the radio during each measurement was manually recorded, and the ranging error was calculated with the aid of computer-aided design (CAD) software. The collected waveforms were then processed to align the first path in the delay domain using a simple threshold-based method. The alignment process creates a time reference independent of the LED algorithm embedded in the radio.

IV. NLOS Identification and Mitigation

The collected measurement data illustrates that NLOS propagation conditions significantly impact ranging performance. For example, Fig. 3 shows the empirical CDFs of the ranging error over the ensemble of all measurements collected under the two different channel conditions. In LOS conditions a ranging error below one meter occurs in more than 95% of the measurements. On the other hand, in NLOS conditions a ranging error below one meter occurs in less than 30% of the measurements.

Clearly, LOS and NLOS range estimates have very different characteristics. In this section, we develop techniques to distinguish between LOS and NLOS situations, and to mitigate the positive biases present in NLOS range estimates. Our techniques are non-parametric, and rely on least-squares support-vector machines (LS-SVM) [47], [48]. We first describe the features for distinguishing LOS and NLOS situations, followed by a brief introduction into LS-SVM. We then describe how LS-SVM can be used for NLOS identification and mitigation in localization applications, without needing to determine parametric joint distributions of the features for both the LOS and NLOS conditions.

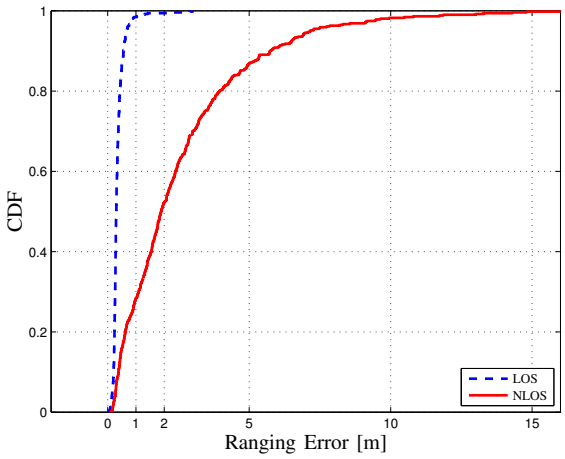

Fig. 3. CDF of the ranging error for the LOS and NLOS condition.

A. Feature Selection for NLOS Classification

We have extracted a number of features, which we expect to capture the salient differences between LOS and NLOS signals, from every received waveform $r(t)$. These features were selected based on the following observations: (i) in NLOS conditions, signals are considerably more attenuated and have smaller energy and amplitude due to reflections or obstructions; (ii) in LOS conditions, the strongest path of the signal typically corresponds to the first path, while in NLOS conditions weak components typically precede the strongest path, resulting in a longer rise time; and (iii) the root-mean-square (RMS) delay spread, which captures the temporal dispersion of the signal's energy, is larger for NLOS signals. Fig. 4 depicts two waveforms received in the LOS and NLOS condition supporting our observations. We also include some features that have been presented in the literature. Taking these considerations into account, the features we will consider are as follows:

1) *Energy of the received signal:*

$$\mathcal{E}_{\mathrm{r}} = \int_{-\infty}^{+\infty} |r(t)|^2 \, dt \tag{2}$$

2) *Maximum amplitude of the received signal:*

$$r_{\max} = \max_{t} |r\,(t)| \tag{3}$$

3) *Rise time:*

$$t_{\mathrm{rise}} = t_{\mathrm{H}} - t_{\mathrm{L}} \tag{4}$$

where

$$t_{\mathrm{L}} = \min\{t : |r(t)| \geq \alpha\sigma_n\}$$
$$t_{\mathrm{H}} = \min\{t : |r(t)| \geq \beta r_{\max}\}\ ,$$

and σ_n is the standard deviation of the thermal noise. The values of $\alpha > 0$ and $0 < \beta \leq 1$ are chosen empirically in order to capture the rise time; in our case, we used $\alpha = 6$ and $\beta = 0.6$.

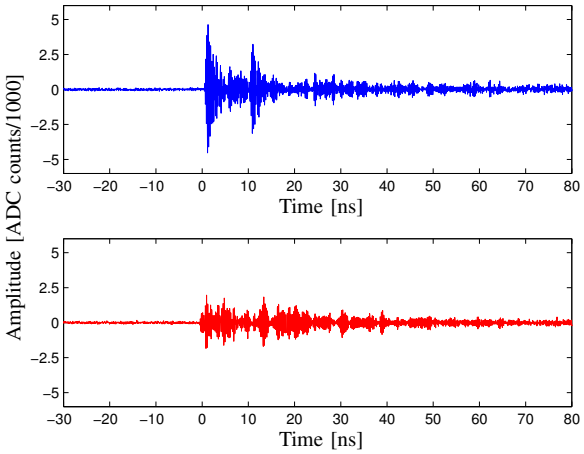

Fig. 4. In some situations there is a clear difference between LOS (upper waveform) and NLOS (lower waveform) signals.

4) *Mean excess delay:*

$$\tau_{\text{MED}} = \int_{-\infty}^{+\infty} t\psi(t)\,dt \tag{5}$$

where $\psi(t) = |r(t)|^2 / \mathcal{E}_{\text{r}}$.

5) *RMS delay spread:*

$$\tau_{\text{RMS}} = \int_{-\infty}^{+\infty} (t - \tau_{\text{MED}})^2 \psi(t)\,dt \tag{6}$$

6) *Kurtosis:*

$$\kappa = \frac{1}{\sigma_{|r|}^4 T} \int_T \left[|r(t)| - \mu_{|r|}\right]^4 dt \tag{7}$$

where

$$\mu_{|r|} = \frac{1}{T}\int_T |r(t)|\,dt$$
$$\sigma_{|r|}^2 = \frac{1}{T}\int_T \left[|r(t)| - \mu_{|r|}\right]^2 dt\,.$$

B. Least Squares SVM

The SVM is a supervised learning technique used both for classification and regression problems [49]. The SVM represents one of the most widely used classification techniques because of its robustness, its rigorous underpinning, the fact that it requires few user-defined parameters, and its superior performance compared to other techniques such as neural networks. LS-SVM is a low-complexity variation of the standard SVM, which has been applied successfully to classification and regression problems [47], [48].

1) Classification: A linear classifier is a function $\mathbb{R}^n \rightarrow \{-1, +1\}$ of the form

$$l(\mathbf{x}) = \text{sign}\left[y(\mathbf{x})\right] \tag{8}$$

with

$$y(\mathbf{x}) = \mathbf{w}^T \varphi(\mathbf{x}) + b \tag{9}$$

where $\varphi(\cdot)$ is a predetermined function, and $\mathbf{w}$ and b are unknown parameters of the classifier. These parameters are determined based on the training set $\{\mathbf{x}_k, l_k\}_{k=1}^N$, where $\mathbf{x}_k \in \mathbb{R}^n$ and $l_k \in \{-1, +1\}$ are the inputs and labels, respectively. In the case where the two classes can be separated the SVM determines the separating hyperplane which maximizes the margin between the two classes.[2] Typically, most practical problems involve classes which are not separable. In this case, the SVM classifier is obtained by solving the following optimization problem:

$$\arg\min_{\mathbf{w},b,\boldsymbol{\xi}} \quad \frac{1}{2}\|\mathbf{w}\|^2 + \gamma\sum_{k=1}^N \xi_k \tag{10}$$
$$\text{s.t.} \quad l_k y(\mathbf{x}_k) \geq 1 - \xi_k, \forall k, \tag{11}$$
$$\xi_k \geq 0, \forall k, \tag{12}$$

where the ξ_k are slack variables that allow the SVM to tolerate misclassifications and γ controls the trade-off between minimizing training errors and model complexity. It can be shown that the Lagrangian dual is a quadratic program (QP) [48, eqn. 2.26]. To further simplify the problem, the LS-SVM replaces the inequality (11) by an equality:

$$\arg\min_{\mathbf{w},b,\mathbf{e}} \quad \frac{1}{2}\|\mathbf{w}\|^2 + \gamma\frac{1}{2}\sum_{k=1}^N e_k^2 \tag{13}$$
$$\text{s.t.} \quad l_k y(\mathbf{x}_k) = 1 - e_k, \forall k. \tag{14}$$

Now, the Lagrangian dual is a linear program (LP) [48, eqn. 3.5], which can be solved efficiently by standard optimization toolboxes. The resulting classifier can be written as

$$l(\mathbf{x}) = \text{sign}\left[\sum_{k=1}^N \alpha_k l_k K(\mathbf{x}, \mathbf{x}_k) + b\right], \tag{15}$$

where α_k, the Lagrange multipliers, and b are found from the solution of the Lagrangian dual. The function $K(\mathbf{x}_k, \mathbf{x}_l) = \varphi(\mathbf{x}_k)^T \varphi(\mathbf{x}_l)$ is known as the kernel which enables the SVM to perform nonlinear classification.

2) Regression: A linear regressor is a function $\mathbb{R}^n \rightarrow \mathbb{R}$ of the form

$$y(\mathbf{x}) = \mathbf{w}^T \varphi(\mathbf{x}) + b \tag{16}$$

where $\varphi(\cdot)$ is a predetermined function, and $\mathbf{w}$ and b are unknown parameters of the regressor. These parameters are determined based on the training set $\{\mathbf{x}_k, y_k\}_{k=1}^N$, where $\mathbf{x}_k \in \mathbb{R}^n$ and $y_k \in \mathbb{R}$ are the inputs and outputs, respectively. The LS-SVM regressor is obtained by solving the following optimization problem:

$$\arg\min_{\mathbf{w},b,\mathbf{e}} \quad \frac{1}{2}\|\mathbf{w}\|^2 + \gamma\frac{1}{2}\|\mathbf{e}\|^2 \tag{17}$$
$$\text{s.t.} \quad y_k = y(\mathbf{x}_k) + e_k, \forall k, \tag{18}$$

where γ controls the trade-off between minimizing training errors and model complexity. Again, the Lagrangian dual is

[2]The *margin* is given by $1/\|\mathbf{w}\|$, and is defined as the smallest distance between the decision boundary $\mathbf{w}^T\varphi(\mathbf{x}) + b = 0$ and any of the training examples $\varphi(\mathbf{x}_k)$.

an LP [48, eqn. 3.32], whose solution results in the following LS-SVM regressor

$$y(\mathbf{x}) = \sum_{k=1}^{N} \alpha_k K(\mathbf{x}, \mathbf{x}_k) + b\,. \tag{19}$$

C. LS-SVM for NLOS Identification and Mitigation

We now apply the non-parametric LS-SVM classifier to NLOS identification, and the LS-SVM regressor to NLOS mitigation. We use 10-fold cross-validation[3] to assess the performance of our features and the SVM. Not only are we interested in the performance of LS-SVM for certain features, but we are also interested in which subsets of the available features give the best performance.

1) Classification: To distinguish between LOS and NLOS signals, we train an LS-SVM classifier with inputs $\mathbf{x}_k$ and corresponding labels $l_k = +1$ when $\lambda_k = \text{LOS}$ and $l_k = -1$ when $\lambda_k = \text{NLOS}$. The input $\mathbf{x}_k$ is composed of a subset of the features given in Section IV-A. A trade-off between classifier complexity and performance can be made by using a different size feature subset.

2) Regression: To mitigate the effect of NLOS propagation, we train an LS-SVM regressor with inputs $\mathbf{x}_k$ and corresponding outputs $y_k = \varepsilon_k$ associated with the NLOS signals. Similar to the classification case, $\mathbf{x}_k$ is composed of a subset of features, selected from those given in Section IV-A and the range estimate $\hat{d}_k$. Again, the performance achieved by the regressor will depend on the size of the feature subset and the combination of features used.

V. Localization Strategies

Based on the LS-SVM classifier and regressor, we can develop the following localization strategies: (i) localization via *identification*, where only classification is employed; (ii) localization via *identification and mitigation*, where the received waveform is first classified and error mitigation is performed only on the range estimates from those signals identified as NLOS; and (iii) a *hybrid* approach which discards mitigated NLOS range estimates when a sufficient number of LOS range estimates are present.

A. Strategy 1: Standard

In the standard strategy, all the range estimates $\hat{d}_i$ from neighboring anchor nodes are used by the LS algorithm (1) for localization. In other words,

$$\mathcal{S}_{\text{S}} = \left\{ \left(\mathbf{p}_i, \hat{d}_i \right) : 1 \le i \le N_{\text{b}} \right\}. \tag{20}$$

[3]In K-fold cross-validation, the dataset is randomly partitioned into K parts of approximately equal size, each containing 50% LOS and 50% NLOS waveforms. The SVM is trained on $K-1$ parts and the performance is evaluated on the remaining part. This is done a total of K times, using each of the K parts exactly once for evaluation and $K-1$ times for training.

TABLE I
False alarm probability (P_{F}), missed detection probability (P_{M}), and overall error probability (P_{E}) for different NLOS identification techniques. The set $\mathcal{F}_{\text{I}}^{i}$ denotes the set of i features with the smallest P_{E} using the LS-SVM technique.

Identification Technique	P_{F}	P_{M}	P_{E}
Parametric technique given in [50]	0.184	0.143	0.164
LS-SVM using features from [50]	0.129	0.152	0.141
$\mathcal{F}_{\text{I}}^{1} = \{r_{\text{max}}\}$	0.137	0.123	0.130
$\mathcal{F}_{\text{I}}^{2} = \{r_{\text{max}}, t_{\text{rise}}\}$	0.092	0.109	0.100
$\mathcal{F}_{\text{I}}^{3} = \{\mathcal{E}_{\text{r}}, t_{\text{rise}}, \kappa\}$	0.082	0.090	0.086
$\mathcal{F}_{\text{I}}^{4} = \{\mathcal{E}_{\text{r}}, r_{\text{max}}, t_{\text{rise}}, \kappa\}$	0.082	0.090	0.086
$\mathcal{F}_{\text{I}}^{5} = \{\mathcal{E}_{\text{r}}, r_{\text{max}}, t_{\text{rise}}, \tau_{\text{MED}}, \kappa\}$	0.086	0.090	0.088
$\mathcal{F}_{\text{I}}^{6} = \{\mathcal{E}_{\text{r}}, r_{\text{max}}, t_{\text{rise}}, \tau_{\text{MED}}, \tau_{\text{RMS}}, \kappa\}$	0.092	0.090	0.091

B. Strategy 2: Identification

In the second strategy, waveforms are classified as LOS or NLOS using the LS-SVM classifier. Range estimates are used by the localization algorithm only if the associated waveform was classified as LOS, while range estimates from waveforms classified as NLOS are discarded:

$$\mathcal{S}_{\text{I}} = \left\{ \left(\mathbf{p}_i, \hat{d}_i \right) : 1 \le i \le N_{\text{b}},\, \hat{\lambda}_i = \text{LOS} \right\}. \tag{21}$$

Whenever the cardinality of $\mathcal{S}_{\text{I}}$ is less than three, the agent is unable to localize.[4] In this case, we set the localization error to $+\infty$.

C. Strategy 3: Identification and Mitigation

This strategy is an extension to the previous strategy, where the received waveform is first classified as LOS or NLOS, and then the mitigation algorithm is applied to those signals with $\hat{\lambda}_i = \text{NLOS}$. For this case $\mathcal{S}_{\text{IM}} = \mathcal{S}_{\text{I}} \cup \mathcal{S}_{\text{M}}$, where

$$\mathcal{S}_{\text{M}} = \left\{ \left(\mathbf{p}_i, \hat{d}_i^{\text{m}} \right) : 1 \le i \le N_{\text{b}},\, \hat{\lambda}_i = \text{NLOS} \right\}, \tag{22}$$

and the mitigated range estimate $\hat{d}_i^{\text{m}}$ is described in Sec. II. This approach is motivated by the observation that mitigation is not necessary for range estimates associated with LOS waveforms, since their accuracy is sufficiently high.

D. Strategy 4: Hybrid Identification and Mitigation

In the *hybrid* approach, range estimates are mitigated as in the previous strategy. However, mitigated range estimates are only used when less than three LOS anchors are available:[5]

$$\mathcal{S}_{\text{H}} = \begin{cases} \mathcal{S}_{\text{I}} & \text{if } |\mathcal{S}_{\text{I}}| \ge 3 \\ \mathcal{S}_{\text{IM}} & \text{otherwise} \end{cases} \tag{23}$$

This approach is motivated by the fact that mitigated range estimates are often still less accurate than LOS range estimates. Hence, only LOS range estimates should be used, unless there is an insufficient number of them to make an unambiguous location estimate.

[4]Note that three is the minimum number of anchor nodes needed to localize in two-dimensions.

[5]In practice the angular separation of the anchors should be sufficiently large to obtain an accurate estimate. If this is not the case, more than three anchors may be needed.

TABLE II
MEAN OF RESIDUAL RANGING ERROR AND RMS RRE FOR LS-SVM REGRESSION-BASED MITIGATION. THE SET $\mathcal{F}_{\mathrm{M}}^{i}$ DENOTES THE SET OF i FEATURES WHICH ACHIEVES THE MINIMUM RMS RRE.

Mitigation Technique with LS-SVM Regression	Mean [m]	RMS [m]
No Mitigation	2.6322	3.589
$\mathcal{F}_{\mathrm{M}}^{1}=\{\hat{d}\}$	-0.0004	1.718
$\mathcal{F}_{\mathrm{M}}^{2}=\{\kappa,\hat{d}\}$	-0.0042	1.572
$\mathcal{F}_{\mathrm{M}}^{3}=\{t_{\mathrm{rise}},\kappa,\hat{d}\}$	0.0005	1.457
$\mathcal{F}_{\mathrm{M}}^{4}=\{t_{\mathrm{rise}},\tau_{\mathrm{MED}},\kappa,\hat{d}\}$	0.0029	1.433
$\mathcal{F}_{\mathrm{M}}^{5}=\{\mathcal{E}_{\mathrm{r}},t_{\mathrm{rise}},\tau_{\mathrm{MED}},\kappa,\hat{d}\}$	0.0131	1.425
$\mathcal{F}_{\mathrm{M}}^{6}=\{\mathcal{E}_{\mathrm{r}},t_{\mathrm{rise}},\tau_{\mathrm{MED}},\tau_{\mathrm{RMS}},\kappa,\hat{d}\}$	0.0181	1.419
$\mathcal{F}_{\mathrm{M}}^{7}=\{\mathcal{E}_{\mathrm{r}},r_{\max},t_{\mathrm{rise}},\tau_{\mathrm{MED}},\tau_{\mathrm{RMS}},\kappa,\hat{d}\}$	0.0180	1.425

VI. PERFORMANCE EVALUATION AND DISCUSSION

In this section, we quantify the performance of the LS-SVM classifier and regressor from Section IV, as well as the four localization strategies from Section V. We will first consider identification, then mitigation, and finally localization. For every technique, we will provide the relevant performance measures as well as the quantitative details of how the results were obtained.

A. LOS/NLOS Identification

Identification results, showing the performance[6] for each feature set size, are given in Table I. For the sake of comparison, we also evaluate the performance of the parametric identification technique from [50], which relies on three features: the mean excess delay, the RMS delay spread, and the kurtosis of the waveform. For fair comparison, these features are extracted from our database. The performance is measured in terms of the misclassification rates $P_{\mathrm{E}}=\left(P_{\mathrm{F}}+P_{\mathrm{M}}\right)/2$, where P_{F} is the false alarm probability (i.e., deciding NLOS when the signal was LOS), and P_{M} is the missed detection probability (i.e., deciding LOS when the signal was NLOS). The table only lists the feature sets which achieved the minimum misclassification rate for each feature set size.

We observe that the LS-SVM, using the three features from [50], reduces the false alarm probability compared to the parametric technique. It was shown in [51] that the features from [50], in fact, give rise to the worst performance among all possible sets of size three considered here. Using the features from Section IV-A and considering all feature set sizes, our results indicate that the feature set of size three, $\mathcal{F}_{\mathrm{I}}^{3}=\{\mathcal{E}_{\mathrm{r}},t_{\mathrm{rise}},\kappa\}$, provides the best performance. Compared to the parametric technique, this set reduces both the false alarm and missed detection probabilities and achieves a correct classification rate of above 91%. In particular, among all feature sets of size three (results not shown, see [51]), there are seven sets that yield a P_{E} of roughly 10%. All seven of these sets have t_{rise} in common, while four have $r_{\max}$ in common, indicating that these two features play an important role. Their importance is also corroborated by the presence of $r_{\max}$ and t_{rise} in the selected sets listed in Table I. For the remainder of this paper we will use the feature set $\mathcal{F}_{\mathrm{I}}^{3}$ for classification.

[6]We have used an RBF kernel of the form $K\left(\mathbf{x},\mathbf{x}_k\right)=\exp\left(-\left\|\mathbf{x}-\mathbf{x}_k\right\|^2\right)$ and set $\gamma=0.1$. Features are first converted to the log domain in order to reduce the dynamic range.

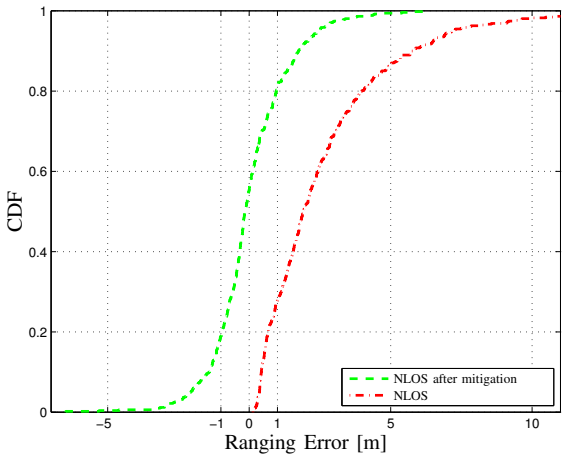

Fig. 5. CDF of the ranging error for the NLOS case, before and after mitigation.

B. NLOS Mitigation

Mitigation results, showing the performance[7] for different feature set sizes are given in Table II. The performance is measured in terms of the root mean square residual ranging error (RMS RRE): $\sqrt{1/N\sum_{i=1}^{N}\left(\varepsilon_i^{\mathrm{m}}\right)^2}$. A detailed analysis of the experimental data indicates that large range estimates are likely to exhibit large positive ranging errors. This means that $\hat{d}$ itself is a useful feature, as confirmed by the presence of $\hat{d}$ in all of the best feature sets listed in the table. Increasing the feature set size can further improve the RMS RRE. The feature set of size six, $\mathcal{F}_{\mathrm{M}}^{6}=\{\mathcal{E}_{\mathrm{r}},t_{\mathrm{rise}},\tau_{\mathrm{MED}},\tau_{\mathrm{RMS}},\kappa,\hat{d}\}$, offers the best performance. For the remainder of this paper, we will use this feature set for NLOS mitigation. Fig. 5 shows the CDF of the ranging error before and after mitigation using this feature set. We observe that without mitigation around 30% of the NLOS waveforms achieved an accuracy of less than one meter ($|\varepsilon|<1$). Whereas, after the mitigation process, 60% of the cases have an accuracy less than 1 m.

C. Localization Performance

1) Simulation Setup: We evaluate the localization performance for fixed number of anchors (N_{b}) and a varying probability of NLOS condition $0\leq P_{\mathrm{NLOS}}\leq 1$. We place an agent at a position $\mathbf{p}=(0,0)$. For every anchor i ($1\leq i\leq N_{\mathrm{b}}$), we draw a waveform from the database: with probability P_{NLOS} we draw from the NLOS database and with probability $1-P_{\mathrm{NLOS}}$ from the LOS database. The true distance d_i corresponding to that waveform is then used to place the ith anchor at position $\mathbf{p}_i=(d_i\sin(2\pi(i-1)/N_{\mathrm{b}}),d_i\cos(2\pi(i-1)/N_{\mathrm{b}}))$, while the estimated distance $\hat{d}_i$ is provided to the agent. This

[7]Here we used a kernel given by $K\left(\mathbf{x},\mathbf{x}_k\right)=\exp\left(-\left\|\mathbf{x}-\mathbf{x}_k\right\|^2/16^2\right)$ and set $\gamma=10$. Again, features are first converted to the log domain.

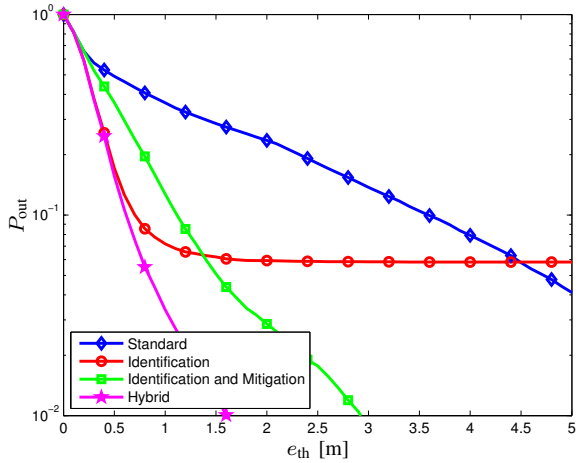

Fig. 6. Outage probability for $N_{\text{b}} = 5$ anchors, with $P_{\text{NLOS}} = 0.2$.

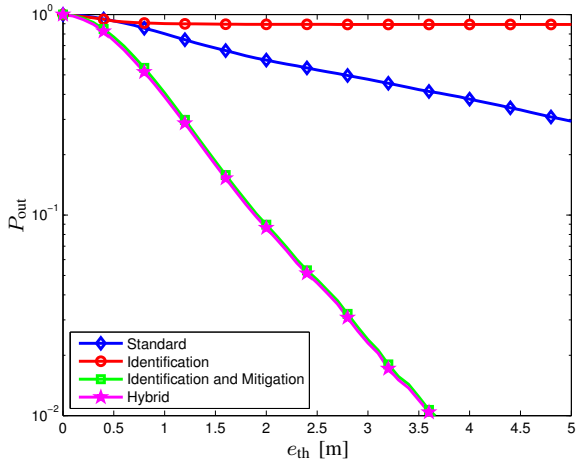

Fig. 7. Outage probability for $N_{\text{b}} = 5$ anchors, with $P_{\text{NLOS}} = 0.8$.

creates a scenario where the anchors are located at different distances from the agent with equal angular spacing. The agent estimates its position, based on a set of useful neighbors $\mathcal{S}$, using the LS algorithm from Section II. The arithmetic mean[8] of the anchor positions is used as the initial estimate of the agent's position.

2) Performance Measure: To capture the accuracy and availability of localization, we introduce the notion of *outage probability*. For a certain scenario (N_{b} and P_{NLOS}) and a certain allowable error e_{th} (say, 2 m), the agent is said to be in outage when its position error $\|\mathbf{p} - \hat{\mathbf{p}}\|$ exceeds e_{th}. The outage probability is then given by

$$P_{\text{out}}\left(e_{\text{th}}\right) = \mathbb{E}\left\{ \mathbb{1}_{\{\|\mathbf{p}-\hat{\mathbf{p}}\| > e_{\text{th}}\}} \right\} , \tag{24}$$

where $\mathbb{1}_{\{\mathcal{P}\}}$ is the indicator function, which, for a proposition $\mathcal{P}$, is zero when $\mathcal{P}$ is false and one otherwise. The outage probability can then be determined through Monte Carlo simulations.

3) Results: Based on the simulation setup described above, we now evaluate the performance with $N_{\text{b}} = 5$ anchors for different values of P_{NLOS}. The outage probability as a function of the allowable error e_{th} for different strategies is plotted in Figs. 6 and 7. The possibility of NLOS anchors can deteriorate the performance as shown in Fig. 6, where $P_{\text{NLOS}} = 0.2$ (corresponding to the scenario where there is, on average, one NLOS anchor). When identification is employed, only the signals identified as LOS are used. We observe that the standard strategy suffers from performance degradation compared to the identification strategy. The identification strategy leads to an error floor phenomenon due to the fact that less than three anchors are available with probability of about 0.06. Identification with mitigation does not suffer from the error floor, since all the anchors are utilized. However this leads to performance degradation for allowable errors below 1.5 m, since the identification with mitigation strategy utilizes all N_{b} anchors, including those identified as NLOS. This may be attributed to the fact that the ranging error is not completely eliminated by this strategy, although it is significantly reduced compared to the standard strategy. The hybrid approach combines the benefits of the previous two strategies, leading to the lowest outage probability for all allowable errors.

[8]This is a fair setting for the simulation, as all the strategies are initialized in the same way. Indeed, despite the identical initialization, strategies converge to significantly different final position estimates. In addition, we note that such an initial position estimate is always available to the agent.

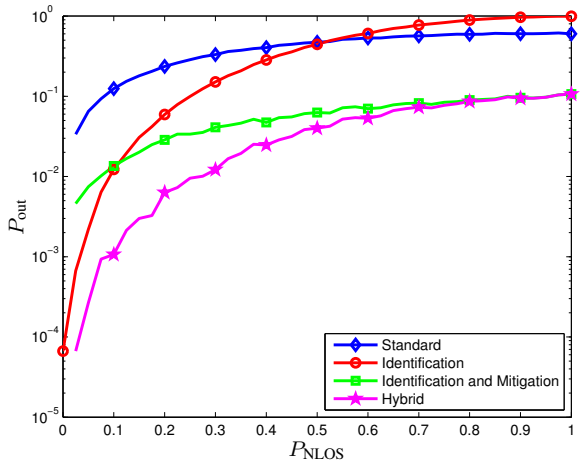

Fig. 8. Outage probability for fixed allowable error $e_{\text{th}} = 2$ m.

When $P_{\text{NLOS}} = 0.8$ (Fig. 7), the identification strategy does not perform well, since the probability that less than three LOS anchors are available is about 0.94. The standard strategy does not fare much better, and both are outperformed by the identification and mitigation strategy. Again, the hybrid strategy leads to the best performance. We observe that as P_{NLOS} tends to one, the latter two strategies will have very similar performance. This is due to the fact that most of the anchors will be in a NLOS condition, yielding $\mathcal{S}_{\text{H}} \approx \mathcal{S}_{\text{IM}}$.

Finally, in Fig. 8, we depict the outage probability as a function of P_{NLOS} for a fixed value of $e_{\text{th}} = 2$ m. The identification strategy is useful only when P_{NLOS} is small, due to the error floor phenomenon. Identification with mitigation dramatically improves the performance, giving an outage prob-

ability of around 10% even when all the anchors are in NLOS. The hybrid approach can further improve the performance, especially when a significant fraction of anchors are in LOS conditions.

VII. Conclusion

In this paper we presented a novel approach that relies solely on features extracted from the received waveform to deal with non-line-of-sight propagation. This technique does not require formulation of explicit statistical models for the features. To validate these techniques in realistic scenarios, we performed an extensive indoor measurement campaign using FCC-compliant UWB radios. We then put forth several features that capture the salient properties of LOS and NLOS signals using our measured waveforms. Based on SVMs, we developed techniques that are capable of distinguishing LOS/NLOS propagation and further mitigating the ranging error in NLOS conditions. Our results revealed that the proposed SVM-based identification technique outperforms previous parametric techniques from the literature. We observe that our non-parametric NLOS identification and mitigation techniques can: (i) deal with highly correlated features without making assumptions about underlying statistical models; and (ii) significantly improve the localization performance in realistic environments.

VIII. Acknowledgment

The authors wish to thank A. Globerson for helpful discussions. The authors also wish to thank U. Ferner, O. Hernandez, P. Pinto, T. Quek, Y. Shen, W. Suwansantisuk, H. Tang, and K. Woradit for their invaluable assistance during the measurement campaign.

References

[1] H. Wymeersch, J. Lien, and M. Z. Win, "Cooperative localization in wireless networks," *Proc. IEEE*, vol. 97, no. 2, pp. 427–450, Feb. 2009, special issue on *Ultra-Wide Bandwidth (UWB) Technology & Emerging Applications*.

[2] N. Patwari, J. N. Ash, S. Kyperountas, A. O. Hero, III, R. L. Moses, and N. S. Correal, "Locating the nodes: cooperative localization in wireless sensor networks," *IEEE Signal Process. Mag.*, vol. 22, no. 4, pp. 54–69, Jul. 2005.

[3] M. Z. Win and R. A. Scholtz, "Impulse radio: How it works," *IEEE Commun. Lett.*, vol. 2, no. 2, pp. 36–38, Feb. 1998.

[4] ——, "On the robustness of ultra-wide bandwidth signals in dense multipath environments," *IEEE Commun. Lett.*, vol. 2, no. 2, pp. 51–53, Feb. 1998.

[5] ——, "On the energy capture of ultra-wide bandwidth signals in dense multipath environments," *IEEE Commun. Lett.*, vol. 2, no. 9, pp. 245–247, Sep. 1998.

[6] ——, "Ultra-wide bandwidth time-hopping spread-spectrum impulse radio for wireless multiple-access communications," *IEEE Trans. Commun.*, vol. 48, no. 4, pp. 679–691, Apr. 2000.

[7] ——, "Characterization of ultra-wide bandwidth wireless indoor communications channel: A communication theoretic view," *IEEE J. Sel. Areas Commun.*, vol. 20, no. 9, pp. 1613–1627, Dec. 2002.

[8] M. Z. Win, "A unified spectral analysis of generalized time-hopping spread-spectrum signals in the presence of timing jitter," *IEEE J. Sel. Areas Commun.*, vol. 20, no. 9, pp. 1664–1676, Dec. 2002.

[9] D. Cassioli, M. Z. Win, and A. F. Molisch, "The ultra-wide bandwidth indoor channel: from statistical model to simulations," *IEEE J. Sel. Areas Commun.*, vol. 20, no. 6, pp. 1247–1257, Aug. 2002.

[10] D. Cassioli, M. Z. Win, F. Vatalaro, and A. F. Molisch, "Low-complexity Rake receivers in ultra-wideband channels," *IEEE Trans. Wireless Commun.*, vol. 6, no. 4, pp. 1265–1275, Apr. 2007.

[11] T. Q. S. Quek, M. Z. Win, and D. Dardari, "Unified analysis of UWB transmitted-reference schemes in the presence of narrowband interference," *IEEE Trans. Wireless Commun.*, vol. 6, no. 6, pp. 2126–2139, Jun. 2007.

[12] A. F. Molisch, D. Cassioli, C.-C. Chong, S. Emami, A. Fort, B. Kannan, J. Karedal, J. Kunisch, H. Schantz, K. Siwiak, and M. Z. Win, "A comprehensive standardized model for ultrawideband propagation channels," *IEEE Trans. Antennas Propag.*, vol. 54, no. 11, pp. 3151–3166, Nov. 2006, special issue on *Wireless Communications*.

[13] D. Dardari, A. Conti, J. Lien, and M. Z. Win, "The effect of cooperation on localization systems using UWB experimental data," *EURASIP J. Appl. Signal Process.*, vol. 2008, pp. Article ID 513 873, 1–11, 2008, special issue on *Cooperative Localization in Wireless Ad Hoc and Sensor Networks*.

[14] H. Wymeersch, U. Ferner, and M. Z. Win, "Cooperative Bayesian self-tracking for wireless networks," *IEEE Commun. Lett.*, vol. 12, no. 7, pp. 505–507, Jul. 2008.

[15] D. B. Jourdan, D. Dardari, and M. Z. Win, "Position error bound for UWB localization in dense cluttered environments," *IEEE Trans. Aerosp. Electron. Syst.*, vol. 44, no. 2, pp. 613–628, Apr. 2008.

[16] J.-Y. Lee and R. A. Scholtz, "Ranging in a dense multipath environment using an UWB radio link," *IEEE J. Sel. Areas Commun.*, vol. 20, no. 9, pp. 1677–1683, Dec. 2002.

[17] D. Dardari, A. Conti, U. J. Ferner, A. Giorgetti, and M. Z. Win, "Ranging with ultrawide bandwidth signals in multipath environments," *Proc. IEEE*, vol. 97, no. 2, pp. 404–426, Feb. 2009, special issue on *Ultra-Wide Bandwidth (UWB) Technology & Emerging Applications*.

[18] C. Falsi, D. Dardari, L. Mucchi, and M. Z. Win, "Time of arrival estimation for UWB localizers in realistic environments," *EURASIP J. Appl. Signal Process.*, vol. 2006, pp. Article ID 32 082, 1–13, 2006, special issue on *Wireless Location Technologies and Applications*.

[19] D. Dardari, C.-C. Chong, and M. Z. Win, "Threshold-based time-of-arrival estimators in UWB dense multipath channels," *IEEE Trans. Commun.*, vol. 56, no. 8, pp. 1366–1378, Aug. 2008.

[20] S. Gezici, Z. Tian, G. B. Giannakis, H. Kobayashi, A. F. Molisch, H. V. Poor, and Z. Sahinoglu, "Localization via ultra-wideband radios: a look at positioning aspects for future sensor networks," *IEEE Signal Process. Mag.*, vol. 22, pp. 70–84, Jul. 2005.

[21] W. Suwansantisuk, M. Z. Win, and L. A. Shepp, "On the performance of wide-bandwidth signal acquisition in dense multipath channels," *IEEE Trans. Veh. Technol.*, vol. 54, no. 5, pp. 1584–1594, Sep. 2005, special section on *Ultra-Wideband Wireless Communications–A New Horizon*.

[22] W. Suwansantisuk and M. Z. Win, "Multipath aided rapid acquisition: Optimal search strategies," *IEEE Trans. Inf. Theory*, vol. 53, no. 1, pp. 174–193, Jan. 2007.

[23] M. Z. Win, P. C. Pinto, and L. A. Shepp, "A mathematical theory of network interference and its applications," *Proc. IEEE*, vol. 97, no. 2, pp. 205–230, Feb. 2009, special issue on *Ultra-Wide Bandwidth (UWB) Technology & Emerging Applications*.

[24] P. C. Pinto, A. Giorgetti, M. Z. Win, and M. Chiani, "A stochastic geometry approach to coexistence in heterogeneous wireless networks," *IEEE J. Sel. Areas Commun.*, vol. 27, no. 7, pp. 1268–1282, Sep. 2009, special issue on *Stochastic Geometry and Random Graphs for Wireless Networks*.

[25] M. Z. Win, G. Chrisikos, and A. F. Molisch, "Wideband diversity in multipath channels with nonuniform power dispersion profiles," *IEEE Trans. Wireless Commun.*, vol. 5, no. 5, pp. 1014–1022, May 2006.

[26] T. Q. S. Quek and M. Z. Win, "Analysis of UWB transmitted-reference communication systems in dense multipath channels," *IEEE J. Sel. Areas Commun.*, vol. 23, no. 9, pp. 1863–1874, Sep. 2005.

[27] M. Z. Win, G. Chrisikos, and N. R. Sollenberger, "Performance of Rake reception in dense multipath channels: Implications of spreading bandwidth and selection diversity order," *IEEE J. Sel. Areas Commun.*, vol. 18, no. 8, pp. 1516–1525, Aug. 2000.

[28] M. Z. Win and Z. A. Kostić, "Virtual path analysis of selective Rake receiver in dense multipath channels," *IEEE Commun. Lett.*, vol. 3, no. 11, pp. 308–310, Nov. 1999.

[29] J. Borras, P. Hatrack, and N. B. Mandayam, "Decision theoretic framework for NLOS identification," in *Proc. 48th Annual Int. Veh. Technol. Conf.*, vol. 2, Ottawa, Canada, May 1998, pp. 1583–1587.

[30] J. Schroeder, S. Galler, K. Kyamakya, and K. Jobmann, "NLOS detection algorithms for ultra-wideband localization," *Positioning, Navigation and Communication, 2007. WPNC '07. 4th Workshop on*, pp. 159–166, Mar. 2007.

[31] S. Gezici, H. Kobayashi, and H. V. Poor, "Non-parametric non-line-of-sight identification," in *Proc. IEEE Semiannual Veh. Technol. Conf.*, vol. 4, Orlando, FL, Oct. 2003, pp. 2544–2548.

[32] I. Guvenc, C.-C. Chong, and F. Watanabe, "NLOS identification and mitigation for UWB localization systems," in *Proc. IEEE Wireless Commun. and Networking Conf.*, Kowloon, China, Mar. 2007, pp. 1571–1576.

[33] F. Benedetto, G. Giunta, A. Toscano, and L. Vegni, "Dynamic LOS/NLOS statistical discrimination of wireless mobile channels," *Vehicular Technology Conference, 2007. VTC2007-Spring. IEEE 65th*, pp. 3071–3075, Apr. 2007.

[34] J. Khodjaev, Y. Park, and A. S. Malik, "Survey of NLOS identification and error mitigation problems in UWB-based positioning algorithms for dense environments," *Annals of Telecommunications*, 2009.

[35] R. Casas, A. Marco, J. J. Guerrero, and J. Falcó, "Robust estimator for non-line-of-sight error mitigation in indoor localization," *EURASIP J. Appl. Signal Process.*, no. 1, pp. 156–156, 2006.

[36] M. Tüchler and A. Huber, "An improved algorithm for UWB-based positioning in a multi-path environment," in *IZS '06: Proceedings of the 2006 International Zürich Seminar on Communications*, 2006, pp. 206–209.

[37] I. Oppermann, M. Hämäläinen, and J. Iinatti, *UWB: Theory and Applications*. Wiley, 2004.

[38] B. Denis and N. Daniele, "NLOS ranging error mitigation in a distributed positioning algorithm for indoor UWB ad-hoc networks," in *International Workshop on Wireless Ad-Hoc Networks*, May/Jun. 2004, pp. 356–360.

[39] S. Venkatesh and R. M. Buehrer, "NLOS mitigation using linear programming in ultrawideband location-aware networks," *IEEE Trans. Veh. Technol.*, vol. 56, no. 5, pp. 3182–3198, Sep. 2007.

[40] S. Venkatraman, J. Caffery, Jr., and H. R. You, "Location using LOS range estimation in NLOS environments," in *Proc. IEEE Semiannual Veh. Technol. Conf.*, vol. 2, Birmingham, Alabama, May 2002, pp. 856–860.

[41] A. Sayed, A. Tarighat, and N. Khajehnouri, "Network-based wireless location: challenges faced in developing techniques for accurate wireless location information," *IEEE Signal Process. Mag.*, vol. 22, no. 4, pp. 24–40, 2005.

[42] S. Al-Jazzar and J. Caffery, Jr., "NLOS mitigation method for urban environments," *Vehicular Technology Conference, 2004. VTC2004-Fall. 2004 IEEE 60th*, vol. 7, pp. 5112–5115, Sep. 2004.

[43] S. Wu, Y. Ma, Q. Zhang, and N. Zhang, "NLOS error mitigation for UWB ranging in dense multipath environments," in *Proc. IEEE Wireless Commun. and Networking Conf.*, Mar. 2007, pp. 1565–1570.

[44] J. Schroeder, S. Galler, K. Kyamakya, and T. Kaiser, "Three-dimensional indoor localization in non line of sight UWB channels," in *Proc. of IEEE Int. Conf. on Ultra-Wideband (ICUWB)*, Singapore, SINGAPORE, Sep. 2007.

[45] Federal Communications Commission, "Revision of part 15 of the commission's rules regarding ultra-wideband transmission systems, first report and order (ET Docket 98-153)," Adopted Feb. 14, 2002, Released Apr. 22, 2002.

[46] H. G. Schantz, "Bottom fed planar elliptical UWB antennas," *Ultra Wideband Systems and Technologies, 2003 IEEE Conference on*, pp. 219–223, Nov. 2003.

[47] J. A. K. Suykens and J. Vandewalle, "Least squares support vector machine classifiers," *Neural Processing Letters*, vol. 9, no. 3, pp. 293–300, Jun. 1999.

[48] J. A. K. Suykens, T. Van Gestel, J. De Brabanter, B. De Moor, and J. Vandewalle, *Least Squares Support Vector Machines*. World Scientific, 2002.

[49] C. Cortes and V. Vapnik, "Support-vector networks," *Machine Learning*, vol. 20, no. 3, pp. 273–297, 1995.

[50] I. Güvenç, C.-C. Chong, F. Watanabe, and H. Inamura, "NLOS identification and weighted least-squares localization for UWB systems using multipath channel statistics," *EURASIP J. on Advances in Signal Processing*, vol. 2008, 2008.

[51] S. Maranò, W. M. Gifford, H. Wymeersch, and M. Z. Win, "Nonparametric obstruction detection for UWB localization," in *Proc. IEEE Global Telecomm. Conf.*, Honolulu, HI, Dec. 2009.